American Mineralogist, Volume 71, pages 136–141, 1986

Cation partitioning in hydrothermally prepared olivine-related (Fe,Mn)-sarcopsides

TORE ERICSSON

Department of Mineralogy and Petrology
Institute of Geology, University of Uppsala
P.O. Box 555, S-75122 Uppsala, Sweden

ANDERS G. NORD AND GÖRAN ÅBERG

Section of Mineralogy, Swedish Museum of Natural History
P.O. Box 50007, S-10405 Stockholm, Sweden

Abstract

Solid solutions of $(Fe_{1-x}Mn_x)_3(PO_4)_2$ ($0 < x \leq 0.20$), with the olivine-related sarcopside structure ($P2_1/a$), have been prepared hydrothermally and analyzed by means of X-ray powder diffraction and ^{57}Fe Mössbauer spectroscopy. The cation sites, M1 and M2, are octahedrally coordinated and are closely related to the corresponding sites in olivine. At 10 K, the solid solutions show magnetic interaction for iron at M2 but no magnetic order at M1. The cations show strong inverse order with Fe^{2+} preferring the M2 site and Mn^{2+} the M1 site, with $K_D(Fe,Mn) \approx 0.2$. A comparison of other phases with sarcopside or olivine structure is made, and a method is described to predict cation partitioning in these structure types.

Introduction

We have recently investigated cation distribution in solid solutions with the olivine structure (e.g., Annersten et al., 1982, 1984; Nord et al., 1982). To supplement these studies, we have now initiated studies on solid solutions with the sarcopside structure, which is closely related to that of olivine (Moore, 1972). Both structures contain two distinct octahedrally coordinated metal cation sites, M1 and M2. Sarcopside-type solid solutions are more easily prepared and equilibrated than the corresponding olivine phases: $(Fe_{1-x}M_x)_3(PO_4)_2$ phases prepared hydrothermally (cf. Kabalov et al., 1973; Ericsson and Nord, 1984) and $(Ni_{1-x}M_x)_3(PO_4)_2$ phases at 1 bar (Nord, 1984). We present here Mössbauer studies of hydrothermally prepared (Fe,Mn)-sarcopsides down to 10 K, primarily to determine cation distributions. We also describe a method to predict cation partitioning in solid solutions with the sarcopside or the olivine structure.

Experimental

Solid solutions with the empirical formula $(Fe_{1-x}Mn_x)_3(PO_4)_2$, (x = 0.05, 0.10, 0.15, . . . , 0.90), were prepared and equilibrated in evacuated and sealed silica tubes at 1070 K as described by Nord and Ericsson (1982). These products are isomorphous with the mineral graftonite, $(Fe,Mn,Ca,Mg)_3(PO_4)_2$, and with $Fe_3(PO_4)_2$ (graftonite phase) which have been described as having 7,5,5- or 6,5,5-coordinated metal sites, respectively (Calvo, 1968; Kostiner and Rea, 1974). $Fe_3(PO_4)_2$-sarcopside was prepared by heating pure Fe-graftonite in a hydrothermal Nimonic-105 autoclave at 800 bar, 570 K for seven days. The synthetic (Fe,Mn)-graftonites were heated hydrothermally at various temperatures and pressures, giving sarcopside phases with $X_{Fe} \leq 0.20$ (cf. Table 1). The phase identification was confirmed by means of X-ray powder diffraction data, obtained with a Guinier-Hägg type focusing camera ($CrK\alpha_1$ radiation, $\lambda = 2.28975$ Å, KCl internal standard).

The ^{57}Fe Mössbauer spectroscopy data were obtained as described by Ericsson and Nord (1984). The centroid shifts (CS) are given in mm/s relative to metallic iron (α-Fe) at room temperature.

Results

X-ray diffraction data

The (Fe,Mn)-sarcopside samples studied crystallize in the monoclinic space group $P2_1/a$, originally determined for a natural sarcopside mineral by Moore (1972). The unit cell parameters are given in Table 1. Other sarcopside phases are also included for comparison. Accurate X-ray powder diffraction data for pure $Fe_3(PO_4)_2$-sarcopside, evaluated with a computer-controlled film scanner (Johansson et al., 1980), are given in Table 2.

The unit cell volumes (Z = 2) are around 300 Å^3. For pure Fe-sarcopside it is 301.2(2) Å^3, i.e., $V/Z = 150.6(1)$ Å^3, which is a curious coincidence with Fe-graftonite, where $V/Z = 150.4(1)$ Å^3 (Kostiner and Rea, 1974). The increase in unit cell volume with Mn substitution is greater for (Fe,Mn)-sarcopsides than for (Fe,Mn)-graftonites. Al-

0003–004X/86/0102–0136$02.00

Table 1. Unit cell dimensions for the hydrothermally prepared $(Fe,Mn)_3(PO_4)_2$ sarcopsides ($P2_1/a$; $Z = 2$). For comparison, data for some other sarcopside phases are included. $(Fe_{0.90}Mn_{0.10})_3$ . . , stands for $(Fe_{0.90}Mn_{0.10})_3(PO_4)_2$ and so forth

Formula	Prepared at p (bar)	t (°C)	a (Å)	b (Å)	c (Å)	β (°)	V (Å^3)	Reference
$Fe_3(PO_4)_2$	800	300	10.442(3)	4.787(1)	6.029(1)	90.98(2)	301.3(2)	This work
$(Fe_{0.90}Mn_{0.10})_3$ [a]	800	300	10.472(8)	4.789(3)	6.045(5)	90.97(7)	303.2(6)	-"-
$(Fe_{0.90}Mn_{0.10})_3$	200	300	10.443(9)	4.808(7)	6.048(4)	90.87(5)	303.6(6)	-"-
$(Fe_{0.80}Mn_{0.20})_3$	800	300	10.494(4)	4.800(1)	6.069(2)	90.79(4)	305.6(3)	-"-
$(Fe_{0.80}Mn_{0.20})_3$	200	300	10.488(5)	4.803(3)	6.064(2)	90.83(3)	305.4(3)	-"-
$(Fe_{0.76}Zn_{0.24})_3$ [b]	-	-	10.404(4)	4.771(3)	6.006(4)	91.12(3)	298.1(3)	Kabalov et al., 1973
$(Fe_{0.20}Mg_{0.80})_3$	30000	500	10.26 (1)	4.75 (1)	5.93 (1)	90.8 (1)	289 (1)	Annersten and Nord, 1980
$(Fe_{0.85}Ni_{0.15})_3$	800	300	10.419(2)	4.757(1)	6.015(1)	90.94(2)	298.1(2)	Ericsson and Nord, 1984
$Ni_3(PO_4)_2$ [c]	1	800?	10.107	4.700	5.830	91.22	276.9	Calvo and Faggiani, 1975
$(Fe_{0.78}Mn_{0.21}Mg_{0.01})_3$ [d]	-	-	10.44 (2)	4.768(9)	6.026(8)	90.0 (1)	299.9(10)	Moore, 1972

a) The "equilibrium" temperatures for the (Fe,Mn)-sarcopsides are only approximate, since the hydrothermal autoclaves could not be quenched but only cooled with air. Cooling rate ~20°/min.

b) Hydrothermally prepared, but p and t not given.

c) Standard deviations not given.

d) Natural mineral

though high temperature and pressure are needed to transform graftonite into sarcopside, it is doubtful whether sarcopside can be regarded as a high pressure phase.

The cell volume increases slightly with respect to $Fe_3(PO_4)_2$-sarcopside with the substitution of the Mn^{2+} ion for Fe^{2+}. The octahedral cation radii are 0.83 and 0.78 Å for divalent high-spin manganese and iron, respectively (Shannon, 1976). The smaller cations (Table 1) imply a corresponding decrease of the unit cell volume, which is experimentally observed for Ni^{2+} ($r^{VI} = 0.69$ Å), Mg^{2+} (0.72 Å), and Zn^{2+} (0.74 Å) (cation radii after Shannon, 1976).

Mössbauer data: paramagnetic region

At room temperature (~295 K) as well as at liquid nitrogen temperature (77 K) the spectra of $(Fe_{1-x}Mn_x)_3(PO_4)_2$ ($0 \leq x \leq 0.20$) are rather similar and consist of two peaks (Fig. 1). At 295 K the high velocity peak is not quite as intense as the low velocity peak but is broader by ~0.02 mm/s. Since peak areas are similar, the asymmetries are not due to textural effects introduced during the absorber preparation (Ericsson and Wäppling, 1976). At 77 K the two peaks are approximately symmetric. The peaks are not broadened by the Mn substitution in the structure, and the hyperfine parameters CS and ΔE_Q are not significantly influenced by variations in Mn/Fe nearest neighbors around the Fe atoms. The Mössbauer parameters at 77 and 295 K are given in Table 3.

CS increases by ~0.13 mm/s for the $Fe_3(PO_4)_2$-sarcopside when the temperature is lowered from 295 to 77 K, which is very likely due to the second order Doppler shift (SOD). The high temperature limit of SOD is $-7.3 \cdot 10^{-4}$ mm·s^{-1}·K^{-1} (Cohen, 1976; p. 27). In addition, ΔE_Q increases by 0.08 mm/s. In the (Fe,Mn)-sarcopsides, ΔE_Q is almost constant when the temperature is lowered from 295 to 77 K; apparently the temperature-induced distortions at M1 and M2 sites are more pronounced in Mn-substituted sarcopsides and almost cancel the expected increase in ΔE_Q at lower temperatures. According to the theory of Ingalls (1964), an increased distortion is expected to cause a decrease in ΔE_Q for Fe^{2+}. From the variations of CS with temperature the metal-oxygen oc-

Table 2. X-ray powder diffraction data for $Fe_3(PO_4)_2$-sarcopside

h	k	l	d_{obs} (Å)	I_{obs}	h	k	l	d_{obs} (Å)	I_{obs}
0	0	1	6.024	35	4	0	1	2.382	8
2	0	0	5.221	2	1	2	0	2.332	12
1	1	0	4.349	10	2	1	-2	2.304	7
2	0	1	3.914	45	4	1	0	2.292	12
0	1	1	3.747	7	2	1	2	2.279	5
2	1	0	3.516	100	1	2	-1	2.177	2
1	1	1			1	2	1	2.172	12
2	1	-1	3.060	8	2	2	-1	2.050	15
0	0	2	3.014	60	2	2	0		
3	1	0	2.816	70	3	1	2	2.043	2
2	0	-2	2.630	4	2	2	1		
4	0	0	2.612	3	0	0	3	2.009	5
2	0	2	2.592	2	0	2	2	1.874	10
3	1	-1	2.564	75	0	1	3	1.853	1
0	1	2	2.550	1	1	1	-3	1.829	30
3	1	1	2.538	15	2	2	-2	1.769	40
1	1	-2	2.486	70	4	2	0	1.764	20
1	1	2	2.470	40	2	2	2	1.758	50
4	0	-1	2.411	1	2	1	3	1.737	10
0	2	0	2.393	10	4	2	1	1.698	2

Guinier-Hägg data ($CrK\alpha_1$ radiation, $\lambda = 2.28975$ Å, KCl internal standard). Monoclinic space group $P2_1/a$, $Z = 2$; $a = 10.442(3)$, $b = 4.787(1)$, $c = 6.029(1)$ Å, $\beta = 90.98(2)°$, $V = 301.3(2)$ Å^3, $M = 357.48$, $d_{calc} = 3.940$ g·cm^{-3}.

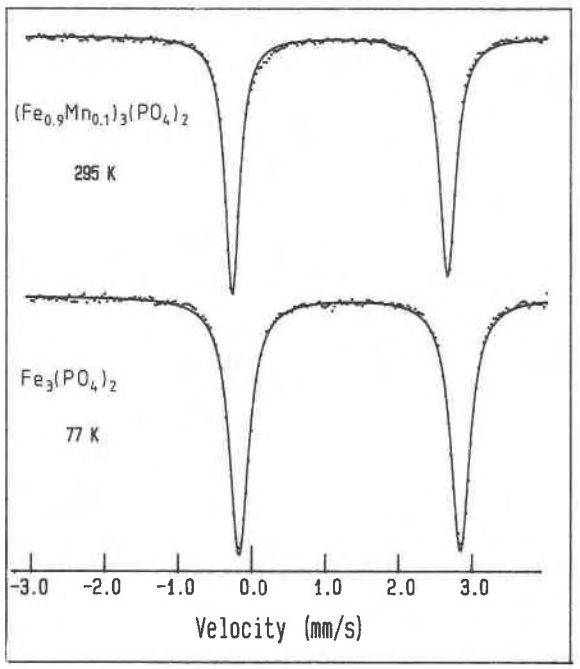

Fig. 1. Mössbauer spectra of $(Fe_{0.90}Mn_{0.10})_3(PO_4)_2$ recorded at 295 K (above) and of $Fe_3(PO_4)_2$-sarcopside at 77 K (below). The solid lines are the sum of the fitted functions.

tahedra apparently contract more when the temperature is lowered for Mn-substituted sarcopsides.

Mössbauer data: magnetically ordered region

The two peaks in the 295 and 77 K spectra (Fig. 1) originate from two overlapping doublets, as in (Ni,Fe)-sarcopsides studied earlier (Ericsson and Nord, 1984). Mössbauer data were collected at ~10 K in order to get resolved patterns containing the crucial information on the cation distribution. There is a magnetic transition at 44 K in $Fe_3(PO_4)_2$-sarcopside. However, only iron at M2 takes part in the magnetic coupling, and the same is true for the (Fe,Mn)-sarcopsides (cf. Fig. 2). The magnetic and electric interactions at M2 are of comparative strengths, even at low temperatures. Accordingly, we have used the full Hamiltonian with theoretical intensities without thickness corrections in the fitting procedure (Jernberg and Sundqvist, 1983). The Mössbauer parameters are listed in Table 4.

One paramagnetic doublet for M1 and one magnetically split set of lines for M2 were used as the fitting model. The actual situation is more complicated in the Mn-substituted sarcopsides, since both sites show very broad lines and the widths increase with increasing Mn content (Table 4; Fig. 2). The reason for this behavior is not obvious, but could be due to local effects like variations in dipolar fields and/or spin cantings as a result of varying numbers of configurations of Fe and Mn neighbors around the Mössbauer atoms. The data in Table 4 are therefore not as accurate as the data in Table 3. In any case, the preference of Mn to substitute for Fe and M1 is quite clear although not as strong as for Ni in the (Ni,Fe)-sarcopsides studied earlier (Ericsson and Nord, 1984).

Table 3. Mössbauer parameters at 77 K and 295 K for $(Fe_{1-x}Mn_x)_3(PO_4)_2$

		Low vel. peak			High vel. peak			Averaged[a]	
Sample	T(K)	Pos.	W	Int.	Pos.	W	Int.	CS	ΔE_Q
$Fe_3(PO_4)_2$	77	-0.17	0.31	0.51	2.85	0.31	0.49	1.34	3.01
	295	-0.26	0.28	0.50	2.67	0.29	0.50	1.21	2.93
$(Fe_{0.9}Mn_{0.1})_3$..	77	-0.16	0.29	0.51	2.74	0.29	0.49	1.29	2.90
	295	-0.25	0.24	0.49	2.68	0.26	0.51	1.21	2.93
$(Fe_{0.8}Mn_{0.2})_3$..	77	-0.16	0.28	0.51	2.73	0.30	0.49	1.29	2.89
	295	-0.21	0.27[b]	0.53[b]	2.66	0.27	0.47	1.22	2.88

a) Averaged values for iron at M1- and M2-sites

b) These values are somewhat increased due to a small (~1 %) Fe^{3+}-impurity in the spectrum

The precision in the fitting procedure is ±0.01 mm/s in positions, widths and CS, ±0.02 mm/s in ΔE_Q and ±0.01 in intensities.

Discussion

Structural features

There is a close structural relationship between olivine and sarcopside (Fig. 3). Olivine (denoted as $M_4(SiO_4)_2$) is orthorhombic (*Pbnm*) with two four-fold, six-coordinated sites M1 and M2 (point symmetries: 1 and *m*). In sarcopside (denoted $M_3\square(PO_4)_2$) the symmetry has been lowered to monoclinic ($P2_1/a$; $\beta \approx 91°$), and the four M1 sites in olivine are split into two two-fold sites, a filled "M1" site and a vacant "□" site; the M2 sites in olivine are preserved as "M2" in sarcopside. M1 and M2 sites in sarcopside are octahedrally coordinated with point symmetries $\bar{1}$ and 1.

All atoms occupy similar positions in the two structures (Fig. 3), and the respective unit cell dimensions are very similar. There are some slight structural differences, e.g., the P-O distances are about 0.1 Å shorter than corresponding Si-O distances. In olivine, the nearly regular MO_6 octahedra are connected in serrated chains, but in sarcopside these chains are broken due to the vacant "□" positions, and instead contain trimers of edge-sharing, slightly distorted MO_6 octahedra (Moore, 1972; cf. Figs. 3, 4).

In both structure types the "$(M2)O_6$" octahedra are slightly larger and display a somewhat larger scatter in metal-oxygen distances and O-M-O angles than "$(M1)O_6$." For example, the average metal-oxygen distances ⟨M1-O⟩ and ⟨M2-O⟩ are 2.095(2) and 2.133(2) Å in Mg_2SiO_4 (Smyth and Hazen, 1973), 2.119(1) and 2.146(1) Å in $Mg_{1.28}Fe_{0.72}SiO_4$ (Wenk and Raymond, 1973), 2.081(2) and 2.084(2) Å in $Ni_3(PO_4)_2$ (Calvo and Faggiani, 1975), 2.11(1) and 2.15(2) Å in $Fe_2Ni(PO_4)_2$ (Ericsson and Nord, 1984), and 2.16(1) and 2.18(1) Å in $(Fe_{0.78}Mn_{0.21}Mg_{0.01})_3(PO_4)_2$ (Moore, 1972). Unfortunately, no structural investigation

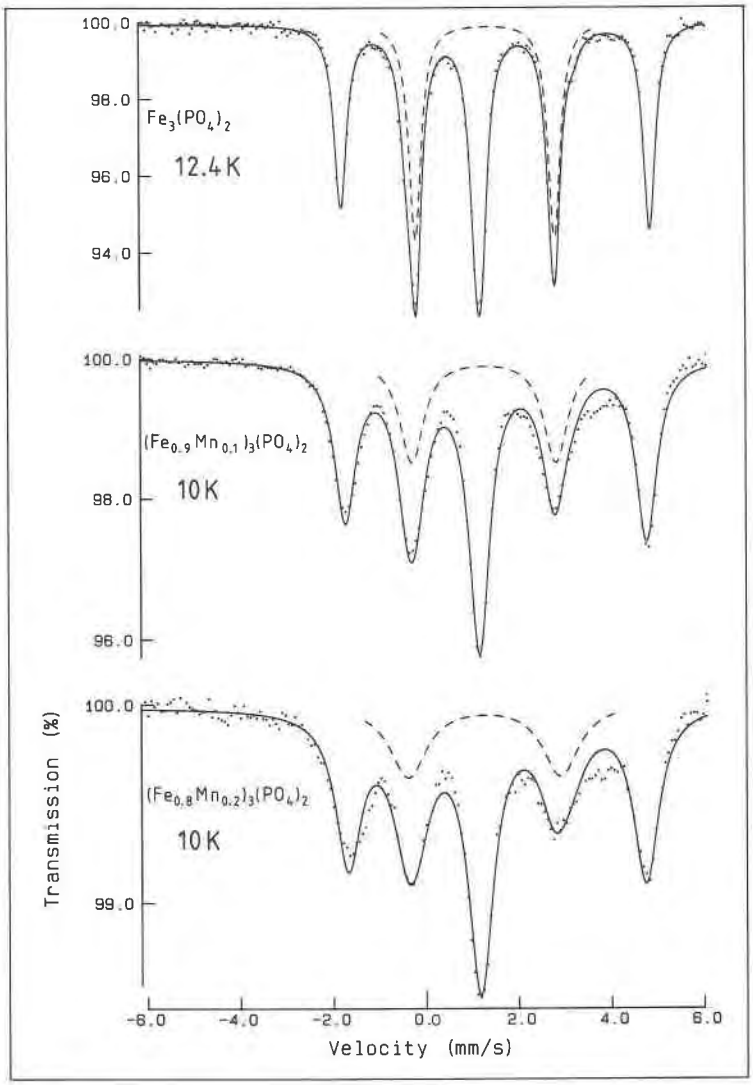

Fig. 2. Mössbauer spectra of $Fe_3(PO_4)_2$-sarcopside, recorded at 12.4 K (above), $(Fe_{0.90}Mn_{0.10})_3(PO_4)_2$ at 10 K (middle), and $(Fe_{0.80}Mn_{0.20})_3(PO_4)_2$ at 10 K (below). The solid lines are the sum of the fitted functions and the dashed lines represent iron at M1.

Table 4. Mössbauer parameters at low temperatures for $(Fe_{1-x}Mn_x)_3(PO_4)_2$ (x = 0.1, 0.2)

			M1: 2-fold, $\bar{1}$-symmetry					M2: 4-fold, 1-symmetry						
Sample	Preparation	T (K)	CS	ΔE_Q[a]	W[b]	Int.	X_{Fe}[c]	CS	ΔE_Q[a]	B[d]	W[b]	Int.	X_{Fe}[c]	K_D[e]
$Fe_3(PO_4)_2$	800 bar/300°C	12.4	1.33	3.02	0.34	0.34	1	1.38	3.11	13.7	0.31	0.66	1	-
$(Fe_{0.9}Mn_{0.1})_3$..	200 bar/300°C	10	1.29	3.13	0.80	0.29	0.79	1.36	3.09	13.2	0.50	0.71	0.95	0.19
$(Fe_{0.9}Mn_{0.1})_3$..	800 bar/300°C	10	1.29	3.18	0.74	0.30	0.81	1.35	3.06	13.0	0.48	0.70	0.94	0.25
$(Fe_{0.8}Mn_{0.2})_3$..	200 bar/300°C	10	1.26	3.40	1.28	0.30	0.72	1.36	3.05	13.0	0.61	0.70	0.84	0.51
$(Fe_{0.8}Mn_{0.2})_3$..	800 bar/300°C	10	1.29	3.41	0.80	0.25	0.60	1.34	3.04	12.8	0.60	0.75	0.90	0.16

a) ΔE_Q is the quadrupole splitting (mm/s) and defined as $\frac{1}{4} \cdot eQV_{zz}\sqrt{1+\eta^2/3}$ for both positions.

b) W is the full width at half maximum (mm/s) of the fitted Lorentzian functions.

c) X_{Fe} is the fraction of the M-sites occupied by iron.

d) B is the hyperfine field and given in Tesla.

e) The cation distribution factor K_D is defined in the text.

The precisions in the fitting procedure are: CS, W = ±0.01, ΔE_Q, Int = ±0.02, B = ±0.1.

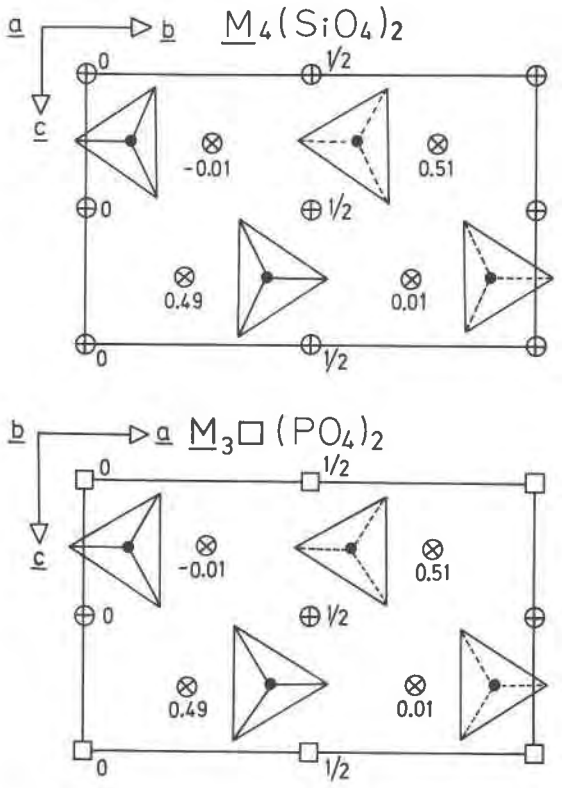

Fig. 3. Projections of the olivine and sarcopside structures, here represented by $M_4(SiO_4)_2$ and $M_3\square(PO_4)_2$. Symbols: ⊕ = M1, ⊗ = M2, □ = vacancy in the sarcopside structure.

of $Fe_3(PO_4)_2$-sarcopside has been undertaken so far, but the above data suggest that in this structure "$(M2)O_6$" is very likely to be the larger octahedron.

Cation distributions and thermodynamical considerations

In a $(Fe,M)_3(PO_4)_2$-sarcopside, the Fe^{2+}/M^{2+} cation distribution can be defined by the equilibrium reaction

$$Fe^{2+}(M2) + M^{2+}(M1) \rightleftharpoons Fe^{2+}(M1) + M^{2+}(M2) \quad (1)$$

The equilibrium constant at the temperature T is given by the expression

$$K_{eq} = [X_{Fe}(M1)\cdot f_{Fe}(M1)\cdot X_M(M2)\cdot f_M(M2)]/[X_{Fe}(M2)\cdot f_{Fe}(M2)\cdot X_M(M1)\cdot f_M(M1)] \quad (2)$$

$X_{Fe}(M1)$ etc. are site occupancy factors, and $f_{Fe}(M1)$ is the partial activity coefficient for divalent iron at M1, etc. If ideal solid solution conditions are assumed to prevail in the (Fe,M)-sarcopsides, the activity coefficients are equal to unity. The cation distribution coefficient K_D is then identical to K_{eq}:

$$K_D(Fe,M) = [X_{Fe}(M1)\cdot X_M(M2)]/[X_{Fe}(M2)\cdot X_M(M1)] \quad (3)$$

Under this assumption, a random distribution of the metal cations is characterized by $K_D = 1$, while $K_D > 1$ shows that Fe^{2+} preferentially enters the M1 sites.

For the hydrothermally prepared (Fe,Mn)-sarcopsides,

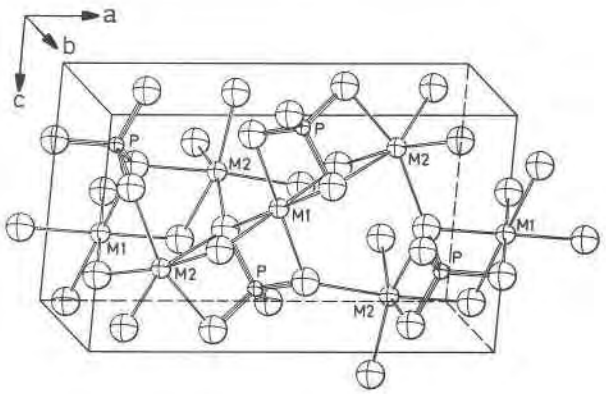

Fig. 4. ORTEP computer drawing of the sarcopside structure, showing an $(M2)O_6$–$(M1)O_6$–$(M2)O_6$ trimer of edge-sharing octahedra.

$K_D(Fe,Mn) \approx 0.2$ (average value; cf. Table 4), indicating a strong *inverse* ordering of Fe^{2+} at the M2 and the larger Mn^{2+} ions at the (presumably) smaller M1 sites. A similar distribution pattern with stronger ordering was found in hydrothermally prepared (Fe,Ni)-sarcopsides, with $K_D(Fe,Ni) \approx 0.01$ (Ericsson and Nord, 1984). From these K_D values, the relevant cations may be arranged in a sequence with respect to their preference for M1 over M2:

$$Ni^{2+} > Mn^{2+} \gg Fe^{2+} \quad (4)$$

Binary $(Ni,M)_3(PO_4)_2$-sarcopsides have been prepared at 1 bar and 1070 K, with the following order of M1-site preference (Nord, 1984):

$$Ni^{2+} > Co^{2+} > Mg^{2+}, Zn^{2+} > Mn^{2+} \gg Fe^{2+} \quad (5)$$

Accordingly, sequence (4) agrees with (5) in spite of different equilibrium conditions and different "base" metals [Fe in (4), and Ni in (5)]. It is therefore worthwhile to estimate a cation distribution coefficient from thermodynamic considerations based on analogous, known K_D values, and the assumption that a K_D value is almost equal to the K_{eq} value in question. For example, $K_D(Fe,Mn)$ in a sarcopside might be estimated from $K_D(Ni,Fe)$ and $K_D(Ni,Mn)$ (Ericsson and Nord, 1984; Nord, 1984) as $K_D(Fe,Mn) \approx K_D(Ni,Mn)/K_D(Ni,Fe) = 6/100 = 0.06$, which is of the same order as the experimental value here reported (~0.2).

This method also seems to be applicable to olivines. For instance, $K_D(Fe,Mn)$ in a $(Fe,Mn)_2SiO_4$ olivine around 1000°C can be estimated from

$$K_D(Fe,Mn) \approx [K_D(Ni,Mn)/K_D(Ni,Fe)] \approx [K_D(Ni,Mg)/K_D(Mn,Mg)]/[K_D(Ni,Fe)] = [9.9/0.196]/[10] \approx 5$$

(data from Bish, 1981; Ghose and Weidner, 1974; Annersten et al., 1982). The experimental K_D value for synthetic (Fe,Mn)-olivine annealed at 1000°C has recently been determined to ~4 (Annersten et al., 1984), so again good agreement is noted.

Mineralogical significance

The K_D(Fe,Mn) values, ~4 for olivine and ~0.2 for sarcopside, show that in olivine the larger cation (Mn^{2+}) is concentrated at the larger site (M2), while the inverse situation is found in sarcopside. Size effects are not significant and the cation partitioning is mainly controlled by crystal field stabilization energies (CFSE) for Fe^{2+} (d^6, a high spin). The divalent manganese ions are in a d^5 high spin configuration having no CFSE. Studies of sarcopside-type solid solutions are therefore a valuable complement to the numerous olivine cation distribution studies reported to date.

Sarcopside as a natural mineral, $(Fe,Mn,Mg)_3(PO_4)_2$, is also of interest, because it has been found terrestrially as well as in meteorites. It is probably an exsolution product since it always seem to be associated with graftonite, $(Fe,Mn,Ca,Mg)_3(PO_4)_2$, or with triphylite, $LiFePO_4$ (Moore, 1972). The amount of manganese is usually less than 25% of the total metal content (cf. Peacor and Garske, 1964; Hurlbut, 1965; Bild, 1974; Fransolet, 1977), which agrees with the solubility limit of our hydrothermally prepared (Fe,Mn)-sarcopsides (~20%). When sarcopside and graftonite occur together in nature, manganese is enriched in the latter phase (Olsen and Fredriksson, 1966), in accordance with the much greater solubility of $Mn_3(PO_4)_2$ in $Fe_3(PO_4)_2$-graftonite, ~90% (Nord and Ericsson, 1982).

Considering the almost identical unit cell volumes of pure Fe-sarcopside and Fe-graftonite, the existence of sarcopside is puzzling. Furthermore, there does not seem to be any need to stabilize either Fe-sarcopside or Fe-graftonite with any other divalent cation. We have, therefore, started further studies of hydrothermal (Fe,M)-sarcopsides in order to shed some light on this problem. Mössbauer studies of natural sarcopside samples might also be worthwhile.

Acknowledgments

We are grateful to Professor Hans Annersten (University of Uppsala) for his kind interest in this project and for many helpful suggestions. Thanks are also due to Professor Peder Kierkegaard (Arrhenius Laboratory, Stockholm) for his permission to use the X-ray diffraction equipment and to Miss Kersti Gløersen for typing the manuscript. This work was funded by the Swedish Natural Science Research Council (NFR).

References

Annersten, H., Adetunji, J., and Filippidis, A. (1984) Cation ordering in Fe-Mn silicate olivines. American Mineralogist, 69, 1110–1115.

Annersten, H., Ericsson, T., and Filippidis, A. (1982) Cation ordering in Ni-Fe olivines. American Mineralogist, 67, 1212–1217.

Annersten, H. and Nord, A. G. (1980) A high pressure phase of magnesium orthophosphate. Acta Chemica Scandinavica, A34, 389–390.

Bild, R. W. (1974) New occurrences of phosphates in iron meteorites. Contributions to Mineralogy and Petrology, 45, 91–98.

Bish, D. L. (1981) Cation ordering in synthetic and natural Ni-Mg olivine. American Mineralogist, 66, 770–776.

Calvo, Crispin (1968) The crystal structure of graftonite. American Mineralogist, 53, 742–750.

Calvo, C. and Faggiani, R. (1975) Structure of nickel orthophosphate. Canadian Journal of Chemistry, 53, 1516–1520.

Cohen, Richard L. (1976) Applications of Mössbauer Spectroscopy, Vol. I. Academic Press, New York.

Ericsson, T. and Nord, A. G. (1984) Strong cation ordering in olivine-related (Ni,Fe)-sarcopsides: a combined Mössbauer, X-ray and neutron diffraction study. American Mineralogist, 69, 889–895.

Ericsson, T. and Wäppling, R. (1976) Texture effects in 3/2-1/2 Mössbauer spectra. Journal de Physique, 37, Colloque C6, 719–723.

Fransolet, André-Mathieu (1977) Intercroissances et inclusions dans les associations graftonite-sarcopside-triphylite. Bulletins de la Société française de Minéralogie et Cristallographie, 100, 198–207.

Ghose, S. and Weidner, J. R. (1974) Site preference of transition metal ions in olivine. Geological Society of America, Abstracts with Programs, 6, 751.

Hurlbut, Jr., C. S. (1965) Detailed description of sarcopside from East Alsted, New Hampshire. American Mineralogist, 50, 1693–1707.

Ingalls, Robert (1964) Electric-field gradient tensor in ferrous compounds. Physical Review, 133A, 787–795.

Jernberg, P. and Sundqvist, T. (1983) A versatile Mössbauer Analysis Program. Uppsala University, Institute of Physics, Report UUIP-1090.

Johansson, K. E., Palm, T., and Werner, P. E. (1980) An automatic microdensitometer for X-ray powder diffraction photographs. Journal of Physics, E13, 1289–1291.

Kabalov, J. K., Simonov, M. A., Jakubovich, O. V., Jamnova, N. A., and Belov, N. V. (1973) Crystal structure of synthetic $(Fe,Zn)_3(PO_4)_2$ sarcopside. Doklady Akademii Nauk SSSR, 210, 830–832 (in Russian).

Kostiner, E. and Rea, J. R. (1974) Crystal structure of ferrous phosphate, $Fe_3(PO_4)_2$. Inorganic Chemistry, 13, 2876–2880.

Moore, P. B. (1972) Sarcopside: its atomic arrangement. American Mineralogist, 57, 24–35.

Nord, A. G. (1984) Crystallographic studies of olivine-related sarcopside-type solid solutions. Zeitschrift für Kristallographie, 166, 159–176.

Nord, A. G., Annersten, H., and Filippidis, A. (1982) The cation distribution in synthetic Mg-Fe-Ni olivines. American Mineralogist, 67, 1206–1211.

Nord, A. G. and Ericsson, T. (1982) The cation distribution in synthetic $(Fe,Mn)_3(PO_4)_2$ graftonite-type solid solutions. American Mineralogist, 67, 826–832.

Olsen, E. and Fredriksson, K. (1966) Phosphates in iron and pallasite meteorites. Geochimica et Cosmochimica Acta, 30, 459–470.

Peacor, D. R. and Garske, D. (1964) Sarcopside from Deering and East Alsted, New Hampshire. American Mineralogist, 49, 1149–1150.

Shannon, R. D. (1976) Revised effective ionic radii and systematic studies of interatomic distances in halides and chalcogenides. Acta Crystallographica, A32, 751–767.

Smyth, J. R. and Hazen, R. M. (1973) The crystal structures of forsterite and hortonolite at several temperatures up to 900°C. American Mineralogist, 58, 588–593.

Wenk, H. R. and Raymond, K. N. (1973) Four new structure refinements of olivine. Zeitschrift für Kristallographie, 137, 86–105.

Manuscript received, February 26, 1985;
accepted for publication, September 4, 1985.